Maximizing the storage capacity of gas networks: a global MINLP approach

Robert Burlacu[1], Herbert Egger[2], Martin Gross[3], Alexander Martin[1], Marc E. Pfetsch[4], Lars Schewe[1], Mathias Sirvent[1], and Martin Skutella[5]

Abstract. In this paper, we study the transient optimization of gas networks, focusing in particular on maximizing the storage capacity of the network. We include nonlinear gas physics and active elements such as valves and compressors, which due to their switching lead to discrete decisions. The former is described by a model derived from the Euler equations that is given by a coupled system of nonlinear parabolic partial differential equations (PDEs). We tackle the resulting mathematical optimization problem by a first-discretize-then-optimize approach. To this end, we introduce a new discretization of the underlying system of parabolic PDEs and prove well-posedness for the resulting nonlinear discretized system. Endowed with this discretization, we model the problem of maximizing the storage capacity as a non-convex mixed-integer nonlinear problem (MINLP). For the numerical solution of the MINLP, we algorithmically extend a well-known relaxation approach that has already been used very successfully in the field of stationary gas network optimization. This method allows us to solve the problem to global optimality by iteratively solving a series of mixed-integer problems (MIPs). Finally, we present two case studies that illustrate the applicability of our approach.

1. Introduction

Optimal control of gas transport networks has become increasingly important in recent years. From a mathematical point of view, this problem results in hard optimization problems that are challenging because they combine nonlinear and discrete aspects. First, we use a model derived from the Euler equations, given by a coupled system of nonlinear parabolic partial differential equations (PDEs). On the other hand, switching active elements such as valves and compressors involves discrete decisions.

In this paper, we consider the particular problem of maximizing the storage capacity of the gas network, which is very important for transmission system operators (TSO).

[1]Friedrich-Alexander-Universität Erlangen-Nürnberg (FAU), Discrete Optimization, Cauerstr. 11, 91058 Erlangen, Germany

[2] Technische Universität Darmstadt, Research Group Numerics and Scientific Computing, Dolivostr. 15, 64293 Darmstadt, Germany

[3] RWTH Aachen, Chair of Management Science, Kackertstr. 7, 52072 Aachen, Germany

[4] Technische Universität Darmstadt, Research Group Optimization, Dolivostr. 15, 64293 Darmstadt, Germany

[5] Technische Universität Berlin, Faculty II – Mathematics and Natural Sciences, Strasse des 17. Juni 136, 10623 Berlin, Germany

Key words and phrases. Mixed-Integer Nonlinear Programming, Transient Gas Transport Optimization, Storage Capacity Maximization, Power-to-Gas, First-Discretize-Then-Optimize.

Especially with regard to *Power-to-Gas* this problem becomes essential. In this context, the gas network is used to store energy by converting electrical power into gas, e.g., by generating hydrogen or methane, and feeding it into the gas network. In a typical Power-to-Gas scenario, the generated gas is only fed into the network during a certain period of time, for example when solar or wind energy is available, and later discharged when demand is high. To handle such scenarios, a transient model of the gas physics is needed, which makes the problem much more complex compared to the stationary case.

In our setting, the problem of maximizing the storage capacity of a gas network is as follows: Maximize the amount of gas that can be fed into the network such that there is an admissible time-dependent control of the active elements satisfying all physical and technical constraints. Furthermore, a concrete control has to be computed. The novel aspect of our contribution is the focus on global optimal solutions while discrete decision are involved. We tackle this global optimization problem by a first-discretize-then-optimize approach. We start with a new discretization of a system of nonlinear parabolic PDEs that describe the gas physics. We prove well-posedness for the resulting discretized system. Incorporating active elements such as valves and compressors, we subsequently obtain a non-convex mixed-integer nonlinear problem (MINLP). In order to to solve this MINLP to global optimality, we algorithmically extend the method proposed by Burlacu et al., 2017; Geißler et al., 2012; Geißler, 2011, which is based on mixed-integer programming (MIP) relaxations of the MINLP and which has already been used successfully in the context of gas network optimization. Finally, two case studies illustrate the applicability of our approach to storage capacity maximization problems. The focus of this paper is to globally maximize the storage capacity of a gas network that includes active elements. To the best of our knowledge, no global optimal approaches have been investigated so far.

Literature review. Several general approaches for optimal control with discrete decisions have been studied in the literature. In the works of H. Lee et al., 1999; Gerdts, 2006, variable time transformation methods that result in a continuous formulation are proposed. However, these are limited to ordinary differential equations (ODEs). Other approaches switch at discrete time points between different systems of ODEs. Recently, a generalization to PDEs was analyzed (Rüffler and F. M. Hante, 2016), whereby only local optimality can be guaranteed. In addition, methods have been developed that use complementarity-based reformulations, see for example the paper by Baumrucker and Biegler, 2009, while they depend on special nonlinear solvers or supplementary relaxation techniques. Recently, Buchheim et al., 2015 presented a global solution method for certain semi-linear elliptic mixed-integer PDE problems using outer approximation. A first-discretize-then-optimize approach has been used in the following articles. Sager, Bock, et al., 2009 developed the so-called convexification method, in which discrete decisions are used to derive a convex relaxation of mixed-integer optimal control problems. This method is limited to ODEs only and is extended to PDEs by F. M. Hante and Sager, 2013. Moreover, Sager, M. Jung, et al., 2011; M. N. Jung et al., 2015 applied this convexification method to handle discrete decisions over time and propose an efficient way to compute feasible solutions. Bock et al., 2018 studied cases in which discrete decisions depend on the state variables and studied a reformulation as well as solution method for such problems. Another direction that has been intensively investigated, especially in the

chemical engineering community, is mixed-integer dynamic optimization. The dynamic system is typically described by a series of differential-algebraic equations (DAEs). Allgor and Barton, 1999 propose a general decomposition-based approach for the problems that arise in this regard. For further surveys in this field of research, we refer to the references contained therein.

In recent years, a lot of literature has been published on optimal control in the context of gas network optimization. The book by Koch et al., 2015 provides a comprehensive survey in case of a *stationary* gas physics. Recently, alternating direction methods have been used (Geißler et al., 2015b; Geißler et al., 2018) to combine MIP and nonlinear programming (NLP) techniques in order to solve stationary gas optimization problems for large-scale real-world instances. Moreover, Ríos-Mercado and Borraz-Sánchez, 2015 as well as F. Hante et al., 2017 present general information on modeling and solution methods for gas transport.

The global optimization of *transient* mixed-integer gas transport has been tackled with related methods by Mahlke et al., 2010 and Domschke, Geißler, et al., 2011. Therein, the authors focus on minimizing the fuel gas consumption of the compressors while gas injection and discharge are given a priori and fixed at each entry and exit. In contrast, we maximize the amount of gas that can be fed into the network, where some entries and exits have a variable gas injection and discharge. Recently, Gugat et al., 2017 presented an instantaneous control approach for solving transient gas transport problems, where an MIP needs to be solved for each time step. Global optimality, however, is only guaranteed for each time step and not for the entire time horizon. Moreover, Hahn et al., 2017 proposed several heuristics for a transient optimal control model for gas transport networks.

2. Mathematical model of gas transport

In this section, we present the basic equations describing the gas transport in a network of pipes and active elements. We start with a description of the topology and geometry of the network and then introduce the partial differential and algebraic equations modeling the conservation of mass and momentum in pipes, active elements, and across junctions.

2.1. Topology and geometry. The topology of the gas network is described by a finite directed graph $\mathcal{G} = (\mathcal{V}, \mathcal{A})$. Every arc $a \in \mathcal{A}$ models a specific segment of the network, i. e. , a pipe or an active element like a compressor or a valve. Correspondingly, we split $\mathcal{A} = \mathcal{A}_{\text{pi}} \cup \mathcal{A}_{\text{ae}}$ into subsets of pipes and active elements. The vertices $v \in \mathcal{V}$, on the other hand, describe the end points of segments and correspond to junctions of several segments or to terminal vertices of the network, where gas can be injected or discharged.

For any vertex $v \in \mathcal{V}$, we denote by $\delta^{\text{in}}(v) := \{a = (v_1, v_2) \in \mathcal{A} : v_2 = v\}$ the set of ingoing arcs and by $\delta^{\text{out}}(v) := \{a = (v_1, v_2) \in \mathcal{A} : v_1 = v\}$ the set of outgoing arcs, and we denote by $\mathcal{A}(v) := \delta^{\text{in}}(v) \cup \delta^{\text{out}}(v)$ the set of arcs that are incident on v. We then split the set of vertices $\mathcal{V} = \mathcal{V}_0 \cup \mathcal{V}_\partial$ into a set of interior vertices $\mathcal{V}_0 := \{v \in \mathcal{V} : |\mathcal{A}(v)| > 1\}$ and a set of boundary vertices $\mathcal{V}_\partial = \{v \in \mathcal{V} : |\mathcal{A}(v)| = 1\}$. We further partition $\mathcal{V}_\partial = \mathcal{V}_q \cup \mathcal{V}_p$ into boundary vertices where either the mass flow or the pressure is prescribed.

To every pipe a, we associate parameters ℓ_a, D_a, and A_a describing the length, diameter, and cross-sectional area of the pipe, and we denote by v_a the midpoint of the pipe corresponding to the arc. We will tacitly identify the pipe a with the interval $[0, \ell_a]$,

which allows us to define differentiation for functions defined on a. In addition, we as-

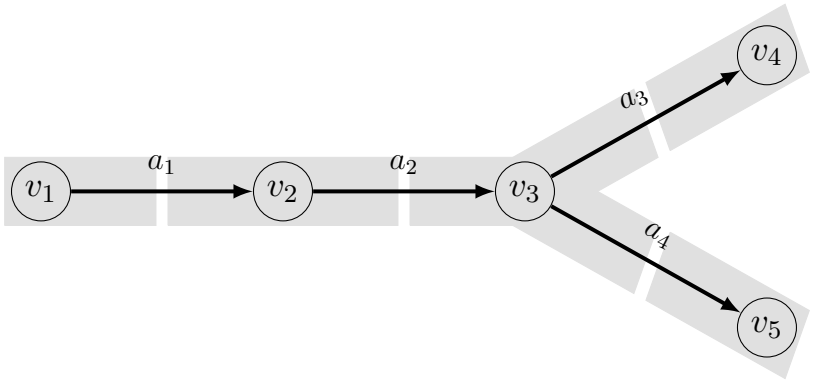

Figure 1. Graph $\mathcal{G} = (\mathcal{V}, \mathcal{A})$ with vertices $\mathcal{V} = \{v_1, v_2, v_3, v_4\}$ and arcs $\mathcal{A} = \{a_1, a_2, a_3, a_4\}$ defined by $a_1 = (v_1, v_2)$, $a_2 = (v_2, v_3)$, $a_3 = (v_3, v_4)$, and $a_4 = (v_3, v_5)$. Here, $\mathcal{V}_0 = \{v_2, v_3\}$ and $\mathcal{V}_\partial = \{v_1, v_4, v_5\}$. Furthermore, we have $\mathcal{A}(v_1) = \{a_1\}$, $\mathcal{A}(v_2) = \{a_1, a_2\}$, $\mathcal{A}(v_3) = \{a_2, a_3, a_4\}$, $\mathcal{A}(v_4) = \{a_3\}$, and $\mathcal{A}(v_5) = \{a_4\}$. Additionally, $\delta^{\text{in}}_{v_1} = \emptyset$, $\delta^{\text{in}}_{v_2} = \{a_1\}$, $\delta^{\text{in}}_{v_3} = \{a_2\}$,$\delta^{\text{in}}_{v_4} = \{a_3\}$, $\delta^{\text{in}}_{v_5} = \{a_4\}$, and $\delta^{\text{out}}_{v_1} = \{a_1\}$, $\delta^{\text{out}}_{v_2} = \{a_2\}$, $\delta^{\text{out}}_{v_3} = \{a_3, a_4\}$, $\delta^{\text{out}}_{v_4} = \emptyset$, $\delta^{\text{out}}_{v_5} = \emptyset$. The control volumes vol_v are shown in gray.

sociate to each vertex $v \in \mathcal{V}$ a control volume vol_v made up of the pipes $a \in \mathcal{A}(v)$ cut to half length, see Figure 1 for an illustration. We refer to the physical volume of these control volumes as $|\text{vol}_v| = \sum_{a \in \mathcal{A}(v)} A_a \ell_a / 2$. We will set $\ell_a > 0$ for pipes and $\ell_a = 0$ for active elements $a \in \mathcal{A}_{\text{ae}}$. Moreover, we require that $\text{vol}_v > 0$ for all $v \in \mathcal{V}$, i. e. , every vertex is end point of at least one pipe $a \in \mathcal{A}_{\text{pi}}$. These topological conditions will be utilized in Section 3. As a next step, we describe the mathematical models for describing the gas flow through pipes and active elements.

2.2. Gas flow through pipes. On the length and time scales that are relevant for the operation of a gas network, the gas transport in a one-dimensional pipe $a \in \mathcal{A}_{\text{pi}}$ is described by the Euler equations, which are given as a system of nonlinear hyperbolic PDEs. They are formed by the Continuity, the Moment, and the Energy Equation; see for example the works of J. Brouwer et al., 2011; A. J. Osiadacz, 1996:

$$\partial_t \rho + \partial_x(\rho v) = 0, \tag{1a}$$

$$\partial_t(\rho v) + \partial_x(p + \rho v^2) = -\frac{\lambda}{2D} \rho v \, |v| - g\rho h', \tag{1b}$$

$$\partial_t\Big(\rho\big(\tfrac{1}{2}v^2 + e\big)\Big) + \partial_x\Big(\rho v\big(\tfrac{1}{2}v^2 + e\big) + pv\Big) = -\frac{k_w}{D}\,(T - T_w)\,. \tag{1c}$$

The three equations (1a)–(1c) describe the conservation of mass, momentum, and energy, respectively. Here, ρ, v, p, and T are the unknown density, velocity, pressure, and temperature, respectively. The constants λ, g, and k_w are the friction coefficient, the gravitational constant, and the heat coefficient. Furthermore, we denote the slope of the pipe by h', the diameter by D, and the temperature at the pipe wall surface by T_w. The internal energy is given by the variable $e = c_v T + gh$ with the specific heat constant c_v and height h of the pipe. System (1) consists of three equations with four unknowns. In

order to complete the system, an additional fourth equation is needed. To this end, we use the Equation of State for real gases

$$p = R_s \rho T z(p, T), \tag{2}$$

where $z(p, T)$ is the compressibility factor and R_s the specific gas constant.

As already mentioned, we put particular emphasis on global optimal solutions of the underlying mathematical optimization problems. As a trade-off, we have to simplify system (1), as is often done in practice. First, we assume that the temperature T is constant, which allows us to neglect the energy equation (1c). The resulting system is often referred to as the isothermal Euler equations. We further assume that the compressibility factor z is constant as well. As a consequence, the speed of sound c can be computed by $c^2 = R_s T z$, which transforms the Equation of State (2) to

$$p = c^2 \rho. \tag{3}$$

Using this, we can rewrite $p + \rho v^2$ as $p\left(1 + v^2/c^2\right)$. In practice, the velocity of the gas is usually significantly lower than the speed of sound in the gas. Typically this is explicitly enforced to prevent noise and vibrations in the pipe. This entails that v^2/c^2 is very small and can therefore be neglected in our model. In addition, we assume that $\partial_t(\rho v)$ is very small as well, see Koch et al., 2015, Chapter 2. This assumption leads to a model comparable to the friction-dominated models discussed by J. Brouwer et al., 2011, which are widely used in the engineering literature for references, see the work of J. Brouwer et al., 2011. For ease of notation, we finally assume that the pipes are horizontal and that the diameter D is constant along pipes. Moreover, we define $q := A\rho v$ as the mass flow, where $A = D^2\pi/4$ is the cross-sectional area of the pipe. Consequently, the Continuity Equation (1a) and the Balance of Moments (1b) simplify to:

$$A\partial_t \rho + \partial_x q = 0, \tag{4}$$

$$\partial_x p = -\frac{\lambda}{2D} \frac{|q|q}{A^2 \rho}. \tag{5}$$

In summary, the system (3)–(5) of nonlinear parabolic PDEs is a friction-dominated approximation of the isothermal Euler equations and the Equation of State (2); see (Domschke, Hiller, et al., 2017) for additional details. In the following, we use system (3)–(5) to represent gas physics.

2.3. Active elements. All active elements in our case are either valves or compressors and can be switched on or off. They denote pipe segments $a = (v_1, v_2) \in \mathcal{A}_{\text{ae}}$ of length $\ell_a = 0$, in which the pressures $p_a(v_1)$, $p_a(v_2)$ and mass flows $q_a(v_1)$, $q_a(v_2)$ at the pipe ends v_1 and v_2 are related in a particular algebraic manner that can be switched between different states. A closed valve or compressor on an arc $a = (v_1, v_2)$ blocks gas from passing, which can be expressed as $q_a(v_2) = q_a(v_1) = 0$. For open valves or compressors in bypass mode, one has $q_a(v_2) = q_a(v_1)$ and $p_a(v_2) = p_a(v_1)$. For an operating compressor, one may assume $q_a(v_2) = q_a(v_1)$ and $p_a(v_2) = p_a(v_1) + \triangle\hat{p}_a$, where $\triangle\hat{p}_a$ is the pressure increase produced by the compressor.

The individual cases mentioned above can be formulated in a unified manner. For an active element $a = (v_1, v_2) \in \mathcal{A}_{\mathrm{ae}}$, the mass and momentum balance is described by

$$q_a(v_1) - q_a(v_2) = 0, \tag{6}$$

$$\hat{s}_a \left(p_a(v_1) - p_a(v_2)\right) + (1 - \hat{s}_a)\, q_a(v_1) = \hat{s}_a \,\hat{\triangle p}_a, \tag{7}$$

where $\hat{s}_a \in \{0, 1\}$ and the pressure increment $\hat{\triangle p}_a$ have to be prescribed. From now on, we use hat symbols to indicate that the corresponding variable is considered as a control or an input data for the gas transport model. Setting $\hat{s}_a = 1$ and choosing $\hat{\triangle p}_a$ appropriately amounts to an open valve or a compressor that is in operating or bypass mode. Choosing $\hat{s}_a = 0$, on the other hand, describes a closed valve or compressor.

After having defined the models for gas transport in pipes and active elements, we now turn to the mathematical models for pipe junctions and terminal vertices.

2.4. Coupling conditions. In order to satisfy the basic conservation principles for mass and momentum also at the interior vertices $v \in \mathcal{V}_0$ of the network, we require that

$$\sum_{a \in \delta^{\mathrm{out}}(v)} q_a(v) - \sum_{a \in \delta^{\mathrm{in}}(v)} q_a(v) = \hat{q}_v, \tag{8}$$

$$p_a(v) = p_v \qquad \text{for all } a \in \mathcal{A}(v). \tag{9}$$

Here, q_a denotes the mass flow in the segment a and $\hat{q}_v$ is a prescribed mass flow entering or leaving the system at the vertex v. The variable p_v denotes the value of the pressure at the vertex v which will be automatically determined when solving the system.

At the boundary vertices $v \in \mathcal{V}_\partial = \mathcal{V}_p \cup \mathcal{V}_q$, we describe either the pressure or mass flow. This can be stated as

$$\sum_{a \in \delta^{\mathrm{out}}(v)} q_a(v) - \sum_{a \in \delta^{\mathrm{in}}(v)} q_a(v) = \hat{q}_v \qquad \text{for all } v \in \mathcal{V}_q, \tag{10}$$

$$p(v) = \hat{p}_v \qquad \text{for all } v \in \mathcal{V}_p. \tag{11}$$

Note that by definition of the boundary vertices, the two sums in (10) only involve one summand. Moreover, the corresponding equations amount to exactly one of the coupling conditions (8) or (9), while the other one is dropped. Again, the hat symbol denotes prescribed data for the gas transport model.

2.5. Initial data. The differential-algebraic system (4)–(11) can formally be reduced to a nonlinear degenerate parabolic system (J. Brouwer et al., 2011). In order to completely describe the evolution of the gas network, one therefore has to additionally prescribe the initial density distribution on all elements $a \in \mathcal{A}$ by

$$\rho_a|_{t=0} = \hat{\rho}_{a,0}. \tag{12}$$

The model (4)–(12) is our complete mathematical model for gas transport on the network and will be the starting point for all further considerations.

3. Discretization

In this section, we will derive a discretization method for the gas transport model discussed in the previous section. We will start with introducing a new variable and a reformulation of the governing equations, which is better suited for a systematic discretization. We then discuss the discretization in space by a finite volume approach on staggered grids and an implicit Euler method. The resulting nonlinear algebraic problem to be solved in each time step can be formulated as a convex minimization problem. This allows to prove the existence and uniqueness of the discretized gas transport problem for a rather general choice of the discrete and continuous controls that serve as input data.

3.1. Change of variables. The equations (3)–(5), which model the gas transport for a single pipe $a \in \mathcal{A}_{\mathrm{pi}}$ can be reformulated equivalently as

$$A_a \partial_t \rho_a + \partial_x q_a = 0, \tag{13}$$

$$\partial_x \pi_a = -\frac{\lambda_a}{D_a} \frac{c^2}{A_a^2} |q_a| q_a, \tag{14}$$

$$\pi_a = c^4 \rho_a^2. \tag{15}$$

Note that, up to scaling, the new variable π_a amounts to the square of the pressure p_a.

Since we only have to consider the cases $\hat{s}_a = 0$ and $\hat{s}_a = 1$, the algebraic equations (6)–(7) modeling the gas transport through active elements $a \in \mathcal{A}_{\mathrm{ae}}$, can be rewritten equivalently as

$$q_a(v_1) = q_a(v_2), \tag{16}$$

$$\hat{s}_a \left(\pi_a(v_1) - \pi_a(v_2)\right) + (1 - \hat{s}_a) q_a(v_1) = \hat{s}_a \, \triangle \hat{\pi}_a, \tag{17}$$

where $\triangle \hat{\pi}_a$ is directly related to $\triangle \hat{p}_a$ via (7).

In a similar manner, we rewrite the coupling conditions (8)–(9) at the interior vertices $v \in \mathcal{V}_0$ as

$$\sum_{a \in \delta^{\mathrm{out}}(v)} q_a(v) - \sum_{a \in \delta^{\mathrm{in}}(v)} q_a(v) = \hat{q}_v, \tag{18}$$

$$\pi_a(v) = \pi_v \qquad \text{for all } a \in \mathcal{A}(v). \tag{19}$$

Again, the value π_v of the squared pressure at the junction v is a variable of the system that has to be determined during the solution process.

Using (3), the boundary conditions (10)–(11) may also be reformulated as

$$\sum_{a \in \delta^{\mathrm{out}}(v)} q_a(v) - \sum_{a \in \delta^{\mathrm{in}}(v)} q_a(v) = \hat{q}_v \qquad \text{for all } v \in \mathcal{V}_q, \tag{20}$$

$$\rho_v = \hat{\rho}_v \qquad \text{for all } v \in \mathcal{V}_p, \tag{21}$$

where $\hat{\rho}_v$ can again be obtained from the prescribed pressure $\hat{p}_v$ via (3). For ease of notation, let us also recall the initial condition

$$\rho_a|_{t=0} = \hat{\rho}_{a,0}. \tag{22}$$

The system (13)–(22) in the three variables ρ, q, and π will be the starting point for the discretization approach outlined in the following.

3.2. Local integral balances. Let us recall that ℓ_a, v_a, and A_a denote the length, midpoint, and cross-sectional area of the arc $a = (v_1, v_2)$, and that vol_v represents the control volume around a vertex v with $|\mathrm{vol}_v| = \sum_{a \in \mathcal{A}(v)} A_a \, \ell_a/2$ denoting the physical volume; see again Figure 1 for an illustration.

By integration of Equation (13) over the control volume vol_v and use of the coupling condition (18) at the vertex v, we obtain

$$\int_{\mathrm{vol}_v} \partial_t \rho \, \mathrm{d}x + \sum_{a \in \delta^{\mathrm{out}}(v)} q_a(v_a) - \sum_{a \in \delta^{\mathrm{in}}(v)} q_a(v_a) = \hat{q}_v. \tag{23}$$

Note that the cross-sectional area A_a from (13) appears implicitly in the definition of the control volume vol_v. Equation (23) expresses the conservation of mass on the control volume vol_v and incorporates the differential equation (13) and the coupling condition (18).

Integration of the momentum equation (14) over a pipe $a = (v_1, v_2)$ leads to

$$\pi_a(v_2) - \pi_a(v_1) = -\frac{\lambda_a}{D_a} \frac{c^2}{A_a^2} \int_a |q_a| q_a \, \mathrm{d}x, \tag{24}$$

which expresses the integral balance of pressure forces and friction over a pipe segment.

For an active element $a = (v_1, v_2)$, we can directly use equation (17), which results in

$$\hat{s}_a \left(\pi_a(v_1) - \pi_a(v_2) \right) + (1 - \hat{s}_a) q_a(v_1) = \hat{s}_a \, \triangle \hat{\pi}_a. \tag{25}$$

This equations resembles the balance of momentum for an active element $a \in \mathcal{A}_{\mathrm{ae}}$.

3.3. Space discretization. We now replace ρ and q by their respective averages over the control volume spaces vol_v and arcs a, which we again denote, by some abuse of notation, by ρ_v and q_a.

As approximation for for integral balance (23) for the conservation of mass over the control volumes vol_v, we then obtain

$$|\mathrm{vol}_v| \, \partial_t \rho_v + \sum_{a \in \delta^{\mathrm{out}}(v)} q_a - \sum_{a \in \delta^{\mathrm{in}}(v)} q_a = \hat{q}_v \qquad \text{for all } v \in \mathcal{V}_0 \cup \mathcal{V}_q. \tag{26}$$

For the boundary vertices $v \in \mathcal{V}_p$, where the pressure is prescribed, we instead require that

$$\rho_v = \hat{p}_v / c^2. \tag{27}$$

On every pipe $a = (v_1, v_2) \in \mathcal{A}_{\mathrm{pi}}$, the balance of momentum is approximately described by

$$\pi_{v_1} - \pi_{v_2} = \ell_a \frac{\lambda_a}{D_a} \frac{c^2}{A_a^2} |q_a| q_a, \tag{28}$$

where the integral in (24) is replaced by $\ell_a |q_a| q_a$, since q_a was approximated by a constant value. In case of active elements $a = (v_1, v_2) \in \mathcal{A}_{\mathrm{ae}}$, we set $\ell_a = 0$ for the calculation of the volume $|\mathrm{vol}_v|$ assigned to the vertex v and replace (28) by

$$\hat{s}_a (\pi_{v_1} - \pi_{v_2}) + (1 - \hat{s}_a) q_a = \hat{s}_a \triangle \hat{\pi}_a.$$

To complete the system, we finally require that

$$\pi_v = c^4 \rho_v^2 \qquad \text{for all } v \in \mathcal{V}. \tag{29}$$

Further, we prescribe the initial density distribution on every control volume vol_v by

$$\rho_v|_{t=0} = \hat{\rho}_{v,0}, \tag{30}$$

where $\hat{\rho}_{v,0}$ may be defined as the average of the initial density distribution $\hat{\rho}_{a,0}$ in (22) over the control volume vol_v. The system (26)–(30) is the numerical model for the gas transport after semi-discretization in space. To obtain a computational model, we still need to discretize in time.

3.4. Time discretization. For the discretization in time, we utilize the implicit Euler method. Let $\tau > 0$ be the time step and let $t_n = n\tau$ with $n = 0, \ldots, N$ denote the discrete time points. For a function u of time, we denote by u_n the approximation for $u(t_n)$ and we use the backward difference quotient $\bar{\partial}_\tau u_n = (u_n - u_{n-1})/\tau$ to approximate the time derivative term $\partial_t u(t_n)$ appearing in equation (26). For ease of notation, let us further define for all $v \in \mathcal{V}$ and all $a \in \mathcal{A}$ the parameters

$$\alpha_v := \frac{|\mathrm{vol}_v|}{\tau} \qquad \text{and} \qquad \beta_a := \frac{\ell_a \lambda_a c^2}{D_a A_a^2}. \tag{31}$$

We further assume that $\hat{s}_{a,n}$, $\hat{\rho}_{v,0}$, $\hat{p}_{v,n}$, $\hat{q}_{v,n}$, and $\triangle\hat{\pi}_{a,n}$ are prescribed. The fully discrete approximation for the gas transport problem (4)–(12) on the network is then given as follows.

Problem 3.1 (Fully discrete problem)**.** Set $\rho_{v,0} = \hat{\rho}_{v,0}$ for $v \in \mathcal{V}$. Then, for $n = 1, \ldots, N$, find solution vectors $\rho_n = (\rho_{v,n})_{v\in\mathcal{V}}$, $q_n = (q_{a,n})_{a\in\mathcal{A}}$, and $\pi_n = (\pi_{v,n})_{v\in\mathcal{V}}$ such that

$$\alpha_v \rho_{v,n} + \sum_{a\in\delta^{\mathrm{out}}(v)} q_{a,n} - \sum_{a\in\delta^{\mathrm{in}}(v)} q_{a,n} = \alpha_v \rho_{v,n-1} + \hat{q}_{v,n} \qquad \text{for all } v \in \mathcal{V}_0 \cup \mathcal{V}_q, \tag{32}$$

$$\alpha_v \rho_{v,n} = \alpha_v \hat{p}_{v,n}/c^2 \qquad \text{for all } v \in \mathcal{V}_p, \tag{33}$$

$$\pi_{v_1,n} - \pi_{v_2,n} = \beta_a |q_{a,n}| q_{a,n} \qquad \text{for all } a = (v_1, v_2) \in \mathcal{A}_{\mathrm{pi}}, \tag{34}$$

$$\hat{s}_{a,n}(\pi_{v_1,n} - \pi_{v_2,n}) + (1 - \hat{s}_{a,n}) q_{a,n} = \hat{s}_{a,n} \triangle\hat{\pi}_{a,n} \qquad \text{for all } a = (v_1, v_2) \in \mathcal{A}_{\mathrm{ae}}, \tag{35}$$

$$\pi_{v,n} = c^2 \rho_{v,n}^2 \qquad \text{for all } v \in \mathcal{V}. \tag{36}$$

Let us note that this problem is a simulation problem that does not involve integer variables, since the controls $\hat{s}_{a,n}$ and $\triangle\hat{\pi}_a$ are assumed to be prescribed here. In the further course of our first-discretize-then-optimize approach, we will deal with optimal control problems where $\hat{s}_{a,n}$ and $\triangle\hat{\pi}_a$ are included as free variables in Section 4. It is not difficult to see that the number of unknowns and equations match, so we can hope for a unique solution once the input and control variables are set appropriately.

3.5. Well-posedness of the fully discrete scheme. Before we proceed to the optimal control problems, let us briefly discuss the well-posedness of Problem 3.1. To do so, it suffices to show that for any $1 \le n \le N$ and given density vector $\rho_{n-1} = (\rho_{v,n-1})_{v\in\mathcal{V}}$, the system (32)–(36) admits a unique solution (ρ_n, q_n, π_n). Recall that the three solution components $\rho_n = (\rho_{v,n})_{v\in\mathcal{V}}$, $q_n = (q_{a,n})_{a\in\mathcal{A}}$, and $\pi_n = (\pi_{v,n})_{v\in\mathcal{V}}$ are vectors containing the respective function values.

3.5.1. *A related minimization problem.* For investigation of the solvability of (32)–(36), we consider the minimization problem

$$\begin{aligned}\min_{\rho_n,q_n,\pi_n} \; & \sum_{v\in\mathcal{V}} \tfrac{c^4\alpha_v}{3}|\rho_{v,n}|^3 + \sum_{a\in\mathcal{A}_{\mathrm{pi}}} \left(\tfrac{\beta_a}{3}|q_{a,n}|^3 - \triangle\hat{\pi}_{a,n}q_{a,n}\right) \\ & + \sum_{a\in\mathcal{A}_{\mathrm{ae}}} \left(\tfrac{1-\hat{s}_{a,n}}{2}|q_{a,n}|^2 - \hat{s}_{a,n}q_{a,n}\triangle\hat{\pi}_{a,n}\right) \end{aligned} \tag{37a}$$

$$\text{s.t.} \quad \alpha_v\rho_{v,n} + \sum_{a\in\delta^{\mathrm{out}}(v)} q_{a,n} - \sum_{a\in\delta^{\mathrm{in}}(v)} q_{a,n} = \alpha_v\rho_{v,n-1} + \hat{q}_{v,n} \qquad \text{for all } v\in\mathcal{V}_0\cup\mathcal{V}_q, \tag{37b}$$

$$\alpha_v\rho_{v,n} = \alpha_v\hat{p}_{v,n}/c^2 \qquad \text{for all } v\in\mathcal{V}_p. \tag{37c}$$

The Lagrangian for this constrained optimization problem reads

$$\begin{aligned} L(\rho_n,q_n,\pi_n) = & \sum_{v\in\mathcal{V}} \tfrac{c^4\alpha_v}{3}|\rho_{v,n}|^3 + \sum_{a\in\mathcal{A}_{\mathrm{pi}}} \left(\tfrac{\beta_a}{3}|q_{a,n}|^3 - \triangle\hat{\pi}_{a,n}q_{a,n}\right) \\ & + \sum_{a\in\mathcal{A}_{\mathrm{ae}}} \left(\tfrac{1-\hat{s}_{a,n}}{2}|q_{a,n}|^2 - \hat{s}_{a,n}q_{a,n}\triangle\hat{\pi}_{a,n}\right) \\ & - \sum_{v\in\mathcal{V}_0\cup\mathcal{V}_q} \pi_{v,n}\Big[\alpha_v\rho_{v,n} + \sum_{a\in\delta^{\mathrm{out}}(v)} q_{a,n} - \sum_{a\in\delta^{\mathrm{in}}(v)} q_{a,n} - \alpha_v\rho_{v,n-1} - \hat{q}_{v,n}\Big] \\ & - \sum_{v\in\mathcal{V}_p} \pi_{v,n}\alpha_v[\rho_{v,n} - \hat{p}_{v,n}/c^2]. \end{aligned}$$

The optimality conditions for the constrained optimization problem are thus given by

$$\begin{aligned} 0 &\overset{!}{=} \partial_{\rho_{v,n}} L(\rho_n,q_n,\pi_n) = c^4\alpha_v|\rho_{v,n}|\rho_{v,n} - \alpha_v\pi_{v,n} && \text{for all } v\in\mathcal{V}, \\ 0 &\overset{!}{=} \partial_{q_{a,n}} L(\rho_n,q_n,\pi_n) = \beta_a|q_{a,n}|q_{a,n} + \pi_{v_2,n} - \pi_{v_1,n} && \text{for all } a=(v_1,v_2)\in\mathcal{A}_{\mathrm{pi}}, \\ 0 &\overset{!}{=} \partial_{q_{a,n}} L(\rho_n,q_n,\pi_n) = (1-\hat{s}_{a,n})q_{a,n} - \hat{s}_{a,n}\triangle\hat{\pi}_{a,n} + \pi_{v_2,n} - \pi_{v_1,n} && \text{for all } a=(v_1,v_2)\in\mathcal{A}_{\mathrm{ae}}, \\ 0 &\overset{!}{=} \partial_{\pi_{v,n}} L(\rho_n,q_n,\pi_n) = \alpha_v\rho_{v,n} + \sum_{a\in\delta^{\mathrm{out}}(v)} q_{a,n} - \sum_{a\in\delta^{\mathrm{in}}(v)} q_{a,n} \\ &\qquad\qquad - \alpha_v\rho_{v,n-1} - \hat{q}_{v,n} && \text{for all } v\in\mathcal{V}_0\cup\mathcal{V}_q, \\ 0 &\overset{!}{=} \partial_{\pi_{v,n}} L(\rho_n,q_n,\pi_n) = -a_v[\rho_{v,n} - \hat{p}_{v,n}/c^2] && \text{for all } v\in\mathcal{V}_p. \end{aligned} \tag{38}$$

It is easy to see that these equations are equivalent to the system (32)–(36), provided that $\rho_v \geq 0$ for all $v\in\mathcal{V}$. Also note that the role of the square pressure $\pi_{v,n}$ is simply that of the Lagrange multiplier of the corresponding constraints (37b) and (37c).

Under some reasonable conditions on the properties of the network, we can now guarantee the existence of a unique solution of the minimization problem (37) for time step $n\in[N] := \{1,\dots,N\}$.

Theorem 3.2. *Let $c>0$, $\alpha_v>0$ for all $v\in\mathcal{V}$, $\beta_a>0$ for all $a\in\mathcal{A}_{\mathrm{pi}}$. Furthermore, let $\rho_{v,n-1}$ and $\hat{s}_{a,n}\in[0,1]$ be given for all $v\in\mathcal{V}$ and $a\in\mathcal{A}_{\mathrm{ae}}$. Then, the problem (37) admits a unique solution.*

Proof. Let us first assume that $\hat{s}_{a,n} \in [0,1)$ for all $a \in \mathcal{A}_{\mathrm{ae}}$. Then the first term of the objective function of the above optimization problem (37) is strictly convex in $\rho = (\rho_v)_{v\in\mathcal{V}}$. The sum of the second and third term is strictly convex in $(q_a)_{a\in\mathcal{A}}$. The constraints (37b)–(37c), on the other hand, are linear and feasible, since $\rho_v \geq 0$ for all $v \in \mathcal{V}$. This already implies the existence of a unique minimizer in the case $\hat{s}_{a,n} \in [0,1)$ for all $a \in \mathcal{A}_{\mathrm{ae}}$.

Now assume that $\hat{s}_{a,n} = 1$ for one arc $a \in \mathcal{A}_{\mathrm{ae}}$. Then from the assumption that $|\mathrm{vol}_v| > 0$, we deduce that one of the vertices v of the active element is connected to a pipe $a' \in \mathcal{A}_{\mathrm{pi}}$. This allows us to formally eliminate the corresponding flow q_a via the linear equation (37b) for v in a pre-processing step, which also makes the Lagrange multiplier π_v superfluous; compare with Equation (38). We are then back in the situation that $\hat{s}_{a,n} < 1$ for all (remaining) $a \in \mathcal{A}_{\mathrm{ae}} \setminus \{a\}$. The case that $\hat{s}_{a,n} = 1$ for several arcs $a \in \mathcal{A}_{\mathrm{ae}}$ can be treated by recursion of the argument. □

3.5.2. *Well-posedness of Problem 3.1.* As mentioned above, as long as $\rho_{v,n} \geq 0$ for all $v \in \mathcal{V}$, the unique solution of the minimization problem (37), which always exists, corresponds to the unique solution of problem (32)–(36). If this is not the case, then problem (32)–(36) does not have a solution. By recursion over n, one can obtain a corresponding statement for the unique solvability of Problem 3.1.

4. The MINLP model

Endowed with the discretization from Section 3, we continue in this section with our first-discretize-then-optimize approach and show how to model the problem of maximizing the storage capacity of gas networks as an MINLP. To obtain a more intuitional modeling, we use a time-expanded graph that can be used equivalently to the fully discretized problem 3.1. Moreover, we incorporate active elements $a \in \mathcal{A}_{\mathrm{ae}} = \mathcal{A}_{\mathrm{vl}} \cup \mathcal{A}_{\mathrm{cm}}$, where $\mathcal{A}_{\mathrm{vl}}$ corresponds to the set of all valves and $\mathcal{A}_{\mathrm{cm}}$ to the set of all compressors, into our model. As mentioned in Subsection 3.4, the control variables $\hat{s}_{a,n}$ and $\triangle\hat{\pi}_a$ are now free and to optimize. We will then consider the solution of this MINLP to global optimality in the succeeding section.

4.1. Pipes. The discretization from Section 3 is a time-expansion technique in which time-dependent properties change only at discrete times. It can therefore be modeled by a time-expanded graph. For this purpose, we copy the gas network for each time point and introduce for each vertex $v \in \mathcal{V}$ an arc (v_n, v_{n+1}) connecting the copy v_n of the vertex v in time step n with the one in time step $n+1$. See Figure 2 for an illustration.

For each vertex $v \in \mathcal{V}$ and time step n we assume lower and upper bounds $p^-_{v,n}$ and $p^+_{v,n}$ for the pressure variable $p_{v,n}$ and lower and upper bounds $q^-_{a,n}$ and $q^+_{a,n}$ for the flow variable $q_{a,n}$ for each arc $a \in \mathcal{A}$ and time step n. With the variable $q_{(v_n,v_{n+1})} := \alpha_v \rho_{v,n}$ and using (32), we now obtain

$$q_{(v_n,v_{n+1})} + \sum_{a\in\delta^{\mathrm{out}}(v)} q_{a,n} - \sum_{a\in\delta^{\mathrm{in}}(v)} q_{a,n} = q_{(v_{n-1},v_n)} + \hat{q}_{v,n} \qquad \text{for all } v \in \mathcal{V}, n \in [N], \quad (39)$$

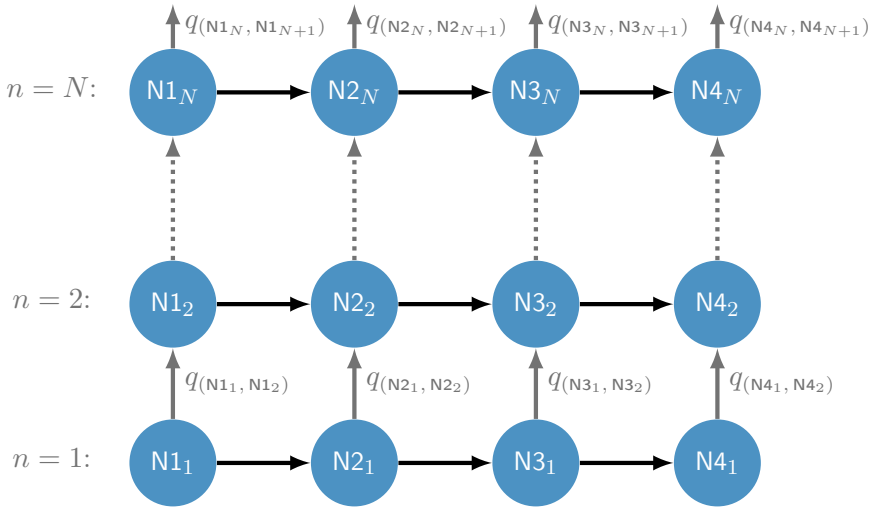

Figure 2. A time-expanded graph of a gas network consisting of 4 vertices N1–N4 and 3 pipes. Each copy of a vertex is linked to the previous and subsequent copies by corresponding arcs (dark gray).

for the flow conservation, where again $[N] = \{1, \dots, N\}$. Since $\pi_{v,n} = p_{v,n}^2$, we can incorporate the pressure loss equation (34) for each pipe $a \in \mathcal{A}_{\text{pi}}$ as

$$p_{v_1(a),n}^2 - p_{v_2(a),n}^2 = \beta_a \, |q_{a,n}| \, q_{a,n} \qquad \text{for all } n \in [N] \tag{40}$$

into our model. Additionally, we have the following equations coupling (39) and (40):

$$q_{(v_n, v_{n+1})} = \alpha_v \, p_{v,n} / c^2 \qquad \text{for all } v \in \mathcal{V}, n \in [N]. \tag{41}$$

We point out that the bounds for $q_{(v_n, v_{n+1})}$ are determined by the bounds for $p_{v,n}$ due to (41). It is also worth noting that this time-expanded graph can be considered as an extension of a stationary pipe model, e. g. , as specified by Fügenschuh et al., 2015, to a transient pipe model.

4.2. Valves. A valve corresponding to arc $a = (v_1, v_2) \in \mathcal{A}_{\text{vl}}$ is modeled using binary variables $s_{a,n} \in \{0, 1\}$ for each time step n, whereby $s_{a,n}$ is equal to one, if and only if the valve is open in time step n and equal to zero for a closed valve. A closed valve blocks gas from passing, which leads to decoupled pressures at vertices v_1 and v_2. For open valves, we have $p_{v_1,n} = p_{v_2,n}$ and thus no pressure loss. This is described by

$$q_{a,n}^- s_{a,n} \le q_{a,n} \le q_{a,n}^+ s_{a,n}, \tag{42a}$$

$$(p_{v_2,n}^+ - p_{v_1,n}^-) s_{a,n} + p_{v_2,n} - p_{v_1,n} \le p_{v_2,n}^+ - p_{v_1,n}^-, \tag{42b}$$

$$(p_{v_1,n}^+ - p_{v_2,n}^-) s_{a,n} + p_{v_1,n} - p_{v_2,n} \le p_{v_1,n}^+ - p_{v_2,n}^-. \tag{42c}$$

4.3. Compressors. Like a valve, a compressor corresponding to arc $a = (v_1, v_2) \in \mathcal{A}_{\text{cm}}$ is modeled via binary variables $s_{a,n} \in \{0, 1\}$ for each time step n, whereby $s_{a,n}$ is equal to one, if and only if the compressor is operating, i. e. , increasing the pressure $p_{v_1,n}$, in time step n. In the following, we restrict ourselves to a simplified compressor model, where an operating compressor may increase the pressure $p_{v_1,n}$ such that

$$1 < r_a^- \leq \frac{p_{v_2,n}}{p_{v_1,n}} \leq r_a^+ \tag{43}$$

holds for given lower and upper bounds r_a^- and r_a^+ of the compression ratio. Note that the flow is only allowed in arc direction (from v_1 to v_2) for an operating compressor with $0 \leq (q_{a,n}^{\text{op}})^- \leq (q_{a,n}^{\text{op}})^+$ as the corresponding bounds. Otherwise, if $s_{a,n}$ is equal to zero, the compressor is in bypass mode, i. e. , we have $p_{v_1,n} = p_{v_2,n}$ while flow in both directions is allowed with the bounds $(q_{a,n}^{\text{by}})^- \leq (q_{a,n}^{\text{by}})^+$. Similar to the paper by Geißler et al., 2015a, we can model this by

$$(q_{a,n}^{\text{by}})^-(1 - s_{a,n}) + (q_{a,n}^{\text{op}})^- s_{a,n} \leq q_{a,n}, \tag{44a}$$

$$(q_{a,n}^{\text{by}})^+(1 - s_{a,n}) + (q_{a,n}^{\text{op}})^+ s_{a,n} \geq q_{a,n}, \tag{44b}$$

$$\triangle_a^- \, s_{a,n} + (p_{v_2,n}^- - p_{v_1,n}^+)(1 - s_{a,n}) \leq p_{v_2,n} - p_{v_1,n}, \tag{44c}$$

$$\triangle_a^+ \, s_{a,n} + (p_{v_2,n}^+ - p_{v_1,n}^-)(1 - s_{a,n}) \geq p_{v_2,n} - p_{v_1,n}, \tag{44d}$$

$$r_a^- \, p_{v_1,n} - (r_a^- \, p_{v_1,n}^+ - p_{v_2,n}^-)(1 - s_{a,n}) \leq p_{v_2,n}, \tag{44e}$$

$$r_a^+ \, p_{v_1,n} - (r_a^+ \, p_{v_1,n}^- - p_{v_2,n}^+)(1 - s_{a,n}) \geq p_{v_2,n}, \tag{44f}$$

where $\triangle_a^-$ and $\triangle_a^+$ are the bounds for the pressure increase. We point out that, unlike the modeling in Section 2, we limit ourselves to compressors that are only in either operating or bypass mode. The possibility to close a compressor can be modeled with an inlet or outlet valve.

4.4. Switching restrictions. Finally, we add constraints to limit switching operations of active elements to predetermined time intervals. These constraints imply that if the status of an active element is changed, then it must stay in this status for a specific time. This is motivated by the practice where the time between changing the settings of the active elements is usually long. In case of a valve, we require that a valve stays closed for S_{vl} seconds if the status is changed from open to closed, and vice versa. We model this for all $a \in \mathcal{A}_{\text{vl}}$ by

$$\sum_{i=n}^{n+M_n-1} s_{a,i} \geq M_n(s_{a,n} - s_{a,n-1}) \qquad \text{for all } n \in [N], \tag{45a}$$

$$\sum_{i=n}^{n+M_n-1} s_{a,i} \leq M_n + M_n(s_{a,n} - s_{a,n-1}) \qquad \text{for all } n \in [N], \tag{45b}$$

where $M_n = \min\{\lceil S_{\text{vl}}/\tau \rceil, \; N - n + 1\}$ considering that the size of a time step τ is given in seconds. In case of a compressor, we require that a compressor stays in bypass mode for S_{cm} seconds if the status changes from operating to bypass, and vice versa. Analogously to a valve, we add (45a) and (45b) with $M_n = \min\{\lceil S_{\text{cm}}/\tau \rceil, \; N - n + 1\}$ for all $a \in \mathcal{A}_{\text{cm}}$ to the model.

4.5. Objective function. We now describe the objective of maximizing the storage capacity of a gas network more formally. To this end, we consider the following situation: Let a nomination $\hat{q}^{\text{nom}} \in \mathbb{R}^{N|\mathcal{V}_\partial|}$ be given, i. e. , supply and demand for each time step n and each terminal vertex $v \in \mathcal{V}_\partial$. We assume that this base load scenario is feasible for the stationary case, i. e. , there exists an admissible configuration of the active elements satisfying all physical and technical constraints in the stationary case; see again (Koch et al., 2015) for more details on this topic. We further assume that such a feasible solution is available.

Moreover, there are time windows $1 \leq k^- \leq k \leq k^+ \leq N$ and $1 \leq l^- \leq l \leq l^+ \leq N$ in which, additionally to the nomination, a positive amount of gas $q^{\text{extra}} \in \mathbb{R}^{N|\mathcal{V}_{st}|}$ can be injected at selected entries $\mathcal{V}_s$ and withdrawn at selected exits $\mathcal{V}_t$, respectively. Lower and upper bounds $(q^{\text{extra}}_{v,n})^-$ and $(q^{\text{extra}}_{v,n})^+$ for each vertex $v \in \mathcal{V}_{st}$ and time step n are also given. We balance q^{extra} by

$$\sum_{v\in\mathcal{V}_s, n\in[N]} q^{\text{extra}}_{v,n} \; - \sum_{v\in\mathcal{V}_t, n\in[N]} q^{\text{extra}}_{v,n} \; = \; 0. \tag{46}$$

Our goal is to maximize this additional amount of gas that can be stored in the network.

This optimization problem can have different globally optimal solutions. We therefore take a simplified version of the minimization of the compressor energy into account, however, with such low costs that it is almost negligible. This gives us optimal solutions that tend to switch on compressors only when necessary. A possible simple formulation of the compressor energy minimization is

$$\min \sum_{a\in\mathcal{A}_{\text{cm}}} \gamma_1 \int p_{v_2(a)}(t) - p_{v_1(a)}(t)\,\mathrm{d}t + \gamma_2\,|\partial_t(p_{v_2(a)}(t) - p_{v_1(a)}(t))|, \tag{47}$$

where $\gamma_1, \gamma_2 > 0$ can be considered as costs and are small in our case. With the pressure increase $\triangle p_{a,n} := p_{v_2(a),n} - p_{v_1(a),n}$ for all compressors $a = (v_1, v_2) \in \mathcal{A}_{\text{cm}}$ and the change of the pressure increase over time $|\triangle p_{a,n} - \triangle p_{a,n-1}|$, the formulation (47) corresponds to

$$\min \sum_{\substack{a\in\mathcal{A}_{\text{cm}},\\ n\in[N]}} \gamma_1\,\triangle p_{a,n} + \gamma_2\,|\triangle p_{a,n} - \triangle p_{a,n-1}| \tag{48}$$

in our MINLP setting. We note that the absolute values in (48) can be eliminated by applying common LP techniques.

Incorporating (48) into the objective function, we are now able to provide the complete problem of maximizing the storage capacity of a gas network as:

$$\max \sum_{\substack{v\in\mathcal{V}_s,\\ n\in[N]}} q_{v,n}^{\text{extra}} - \sum_{\substack{a\in\mathcal{A}_{\text{cm}},\\ n\in[N]}} \gamma_1 \triangle p_{a,n} + \gamma_2 \left|\triangle p_{a,n} - \triangle p_{a,n-1}\right| \tag{49a}$$

$$\text{s.t. pipe model constraints (39)–(41)}, \tag{49b}$$

$$\text{active elements constraints (42) and (44)}, \tag{49c}$$

$$\text{switching conditions (45)}, \tag{49d}$$

$$\text{flow balance constraint (46)}, \tag{49e}$$

$$p_{v,n}^- \le p_{v,n} \le p_{v,n}^+ \qquad \text{for all } v \in V,\ n \in [N], \tag{49f}$$

$$q_{a,n}^- \le q_{a,n} \le q_{a,n}^+ \qquad \text{for all } a \in \mathcal{A},\ n \in [N], \tag{49g}$$

$$(q_{v,n}^{\text{extra}})^- \le q_{v,n}^{\text{extra}} \le (q_{v,n}^{\text{extra}})^+ \qquad \text{for all } v \in \mathcal{V}_{st},\ n \in [N], \tag{49h}$$

$$s_{a,n} \in \{0,1\} \qquad \text{for all } a \in \mathcal{A}_{\text{ae}},\ n \in [N]. \tag{49i}$$

The nonlinear parts of the MINLP model (49) are given by the pressure loss equations (40) for all $n \in [N]$. Due to these equations this MINLP problem is non-convex. For each $n \in [N]$, the control variables are the binary variables $s_{a,n}$ for all $a \in \mathcal{A}_{\text{cm}} \cup \mathcal{A}_{\text{vl}}$ and the pressure increase $\triangle p_{a,n} := p_{v_2(a),n} - p_{v_1(a),n}$ for all $a \in \mathcal{A}_{\text{cm}}$.

5. Computational results

We now illustrate the applicability of our approach to storage capacity maximization problems by presenting two case studies based on the GasLib-11 (see Figure 3) network; see (Schmidt et al., 2017).

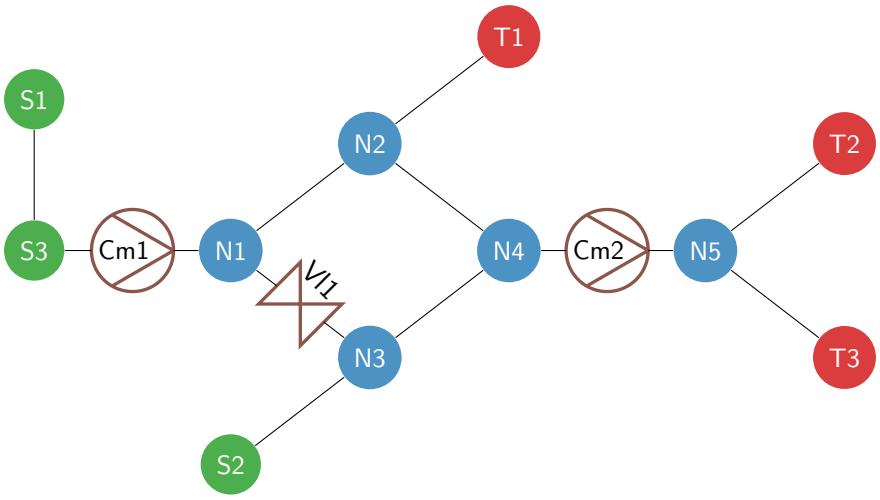

Figure 3. The GasLib-11 network.

The GasLib-11 network depicted in Figure 3 consists of three entries S1–S3, five interior vertices N1–N5, and three exits T1–T3. Two compressors Cm1 and Cm2 are installed

between S3 and N1, and N4 and N5, respectively. We have lower and upper bounds $r_a^- = 1.0895$ and $r_a^+ = 1.6009$ for the compression ratio of both compressors. All eight pipes have a length ℓ_a of 55 km, a diameter D_a of 0.5 m, and a roughness of 0.1 mm resulting in a friction factor $\lambda_a = 0.0137$. The two vertices T1 and T2 have a lower pressure bound of 40 bar and an upper pressure bound of 60 bar. All other vertices have lower and upper pressure bounds of 40 bar and 70 bar. In addition, a valve Vl1 between N1 and N3 is included.

5.1. Solving MINLPs by MIP relaxations. As previously shown, we can model the problem of maximizing the storage capacity of gas networks as an MINLP using (49). There is a wide variety of algorithms to solve MINLPs, for an overview see, e. g. , the works of J. Lee and Leyffer, 2012; Belotti et al., 2013.

In this paper, we consider the method proposed by Burlacu et al., 2017; Geißler et al., 2012; Geißler, 2011, where MINLPs are solved to global optimality by solving a series of mixed-integer linear programs (MIPs). The main idea is to use piecewise linear functions to construct MIP relaxations of the underlying MINLP. In order to find a global optimum, an iterative algorithm is developed that solves MIP relaxations, which are refined adaptively. Additionally, whenever a feasible solution of an MIP relaxation is found, all discrete variables of the MINLP are fixed according to the corresponding solution of the MIP relaxation. Solving the resulting NLP to local optimality often delivers feasible solutions for the MINLP.

The motivation for using this method is as follows. As mentioned in Section 4, we can treat the instationary pipe model derived in the first sections as an extension of a stationary pipe model by a time-expanded graph. Burlacu et al., 2017 present promising numerical results for stationary gas transport optimization, where the MIP relaxation approach outperforms state-of-the-art black box MINLP solvers like Baron (Tawarmalani and Sahinidis, 2005) and SCIP (Gamrath et al., 2016).

We give some insight into the chosen parameters and refer to the references already mentioned for further details on the algorithm. We use 50 bar as error bound for the pressure loss equation (41) in the initial MIP relaxation. Moreover, only those relaxations of the pressure loss equations (41) are chosen for refinement that have a relaxation error larger than 0.85η, where η is the maximum of all relaxation errors.

We highlight two algorithmic extensions to the MIP-based solution method. First, whenever a feasible solution of the MINLP is obtained, we can obviously transform it into a feasible starting solution of the MIP relaxation. This can sometimes reduce the runtime needed to solve the MIP. Furthermore, any objective value of a solution of an MIP relaxation provides a dual bound for the MINLP problem. At the same time, the dual bounds that we obtain while solving an MIP relaxation are also dual bounds for the MINLP. We exploit this by solving a very fine MIP relaxation. Although the MIP solver is unlikely to solve the fine MIP relaxation within reasonable time limits, if a tighter dual bound is found, we can use it as dual bound for the MINLP.

All computations are carried out utilizing this MIP-based approach within the C++ software framework LaMaTTO++, 2015, on a cluster using 12 cores of a machine with two Xeon 5650 Westmere chips running at 2.66 GHz with 24 GB of RAM. Furthermore, we use Gurobi (version 6.0.4 (Gu et al., 2015)) as MIP solver and CONOPT3, provided by GAMS (version 24.8.3 (GAMS, 2017)), as the local NLP solver both within LaMaTTO++.

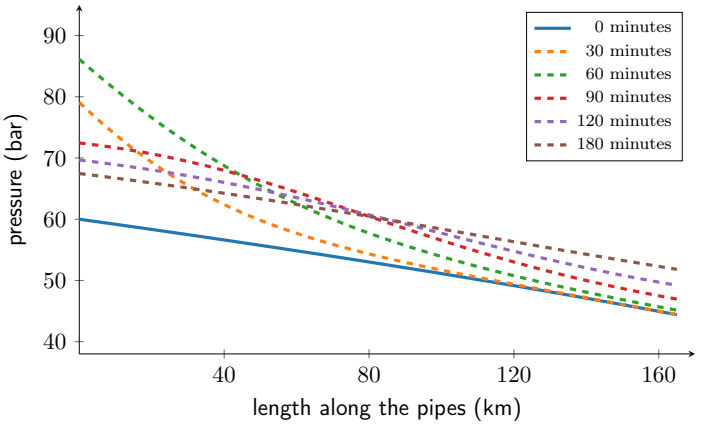

(a) Values for the fine discretization

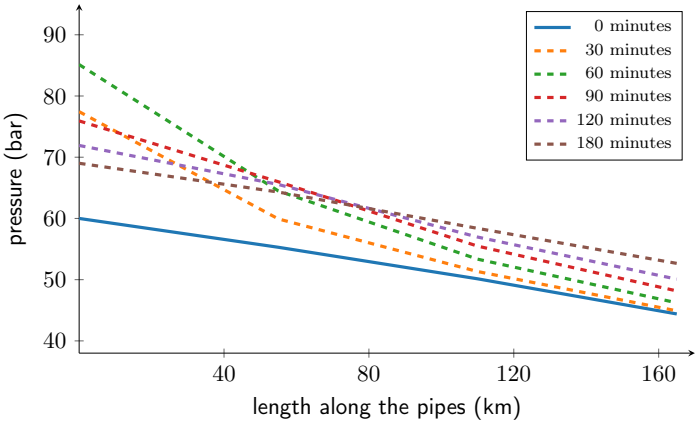

(b) Values for the coarse discretization

Figure 4. Pressure values (y-axis) for a fine (above) and coarse (below) discretization in three consecutive pipes of the GasLib-11 network over their accumulated length (x-axis) for different time points.

5.2. Pressure and flow waves within pipes. As as first case study, we investigate the propagation of pressure and flow waves within pipes. For this purpose, we consider three consecutive pipes from the GasLib-11 network, e. g. , S2–N3–N4–N2, resulting in a total length of 165 km. Initially, we assume a stationary state, where $150\,\mathrm{m}^3\,\mathrm{h}^{-1}$ are injected in S2 and discharged at N2. We immediately increase the supply at S2 to $450\,\mathrm{m}^3\,\mathrm{h}^{-1}$ and inject this amount up to minute 60. From minute 60 on, $150\,\mathrm{m}^3\,\mathrm{h}^{-1}$ are injected again. We choose a time discretization of 5 s and a spatial discretization of 500 m.

The figures 4a and 5a show that our time-expanded graph model is capable of detecting parabolic pressure and flow waves and their propagation within pipes. Furthermore, we notice that although our model is not designed to accurately represent rapid flow changes in time, they are quickly smoothed. This behavior is typical for parabolic equations.

We now give some insight into the discretization of Section 5.3. Therein, we consider a time discretization of 10 min and a two point space discretization of 55 km for the pipes. This coarse discretization is due to the fact that non-convex MINLPs as in (49) are hard

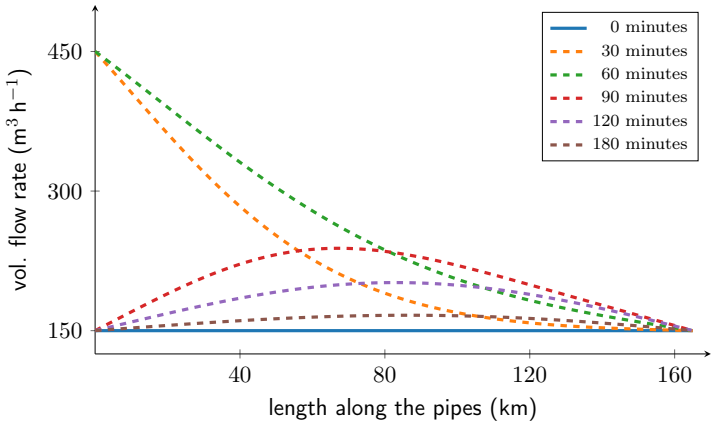

(a) Values for the fine discretization

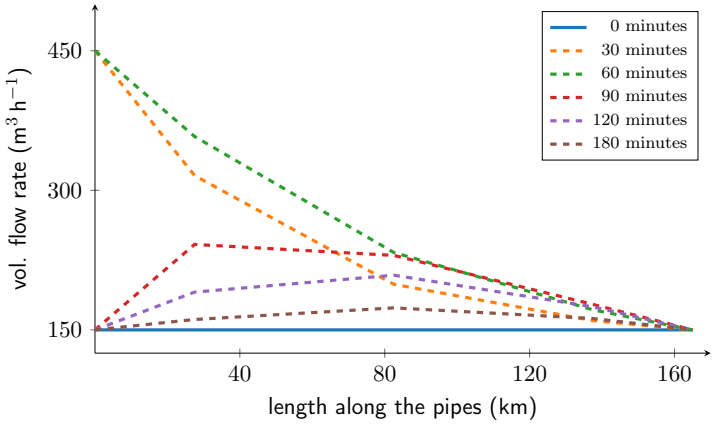

(b) Values for the coarse discretization

Figure 5. Flow values (y-axis) for a fine (above) and coarse (below) discretization in three consecutive pipes of the GasLib-11 network over their accumulated length (x-axis) for different time points.

to solve in general. Hence, we are forced to use a coarse discretization in order to keep the MINLP computationally tractable.

We run the same simulation as before, albeit with the coarse discretization. Analogously, we depict the result for the coarse discretization at different time points in the figures 4b and 5b. Comparing both discretizations, we can observe that the characteristic behavior of the fine discretization is maintained by the coarser one. In addition, the difference between the two discretizations vanishes with large time horizons. With the goal of global optimization, we are therefore confident to use the coarse discretization on time horizons of several hours.

5.3. Storage capacity maximization. As a second case study, we solve the storage capacity maximization problem (49) using the GasLib-11 network shown in Figure 3. We choose the parameters $\gamma_1 = 0.0015$, $\gamma_2 = 0.02$, $S_{\mathrm{cm}} = 7200$, and $S_{\mathrm{vl}} = 3600$, which are

introduced in Section 4. For the prescribed nomination $\hat{q}^{\mathrm{nom}} \in \mathbb{R}^{N|\mathcal{V}_\partial|}$, we use the values that are given in Table 1 for all time steps.

Table 1. The prescribed nomination $\hat{q}^{\mathrm{nom}}$ (given in $\mathrm{m}^3\,\mathrm{h}^{-1}$) for one time step and all entries and exits of the GasLib-11 network.

S1	S2	S3	T1	T2	T3
140.00	160.00	0.00	90.00	150.00	60.00

Both compressors Cm1 and Cm2 run in bypass mode at the beginning while the valve Vl1 is closed, which results in a tree structured network. Thus, we can compute an initial stationary solution by fixing the pressure for S1 to 58 bar and propagation of the flow throughout the network. The resulting initial pressure values for all eleven vertices are given in Table 2.

Table 2. Initial pressure values (given in bar) for all eleven vertices of the GasLib-11 network as in Figure 3.

S1	S2	S3	N1	N2	N3	N4	N5	T1	T2	T3
58.00	59.94	53.77	53.77	49.18	54.55	48.56	48.56	47.15	42.60	47.66

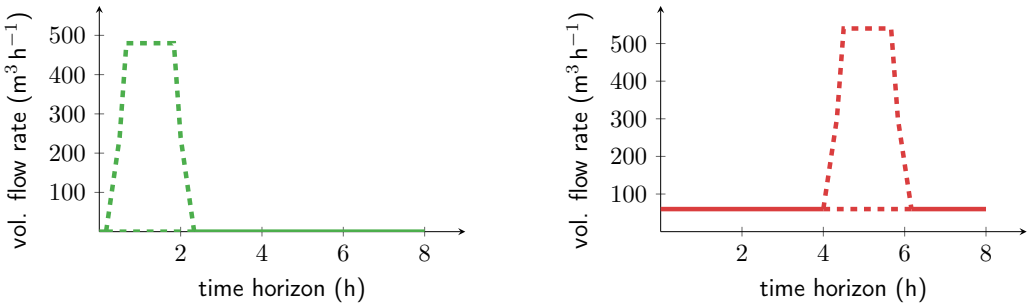

Figure 6. Given volumetric flow rate profiles for the additional amount of gas that can be injected at S3 (left) and must be discharged accordingly at T3 (right). Based on q^{extra} in (49), the dashed lines indicate the additional amount of gas that can be injected at S3 (green lines) and must be discharged accordingly at T3 (red lines) with corresponding upper and lower bounds.

We now consider a time horizon of 8 h, with a time discretization of 10 min leading to a total amount of 48 time steps and a two point space discretization for the pipes. From minute 20 on, a positive amount of gas can be injected for two hours, in addition to the nomination, at S3. We allow a maximal additional amount that corresponds to $500\,\mathrm{m}^3\,\mathrm{h}^{-1}$. Moreover, we stipulate a linear increase (and decrease) in the additionally injectable gas amount up to (and from) the maximum within 20 min. From the fourth hour, the same additional amount of gas must be discharged at T3 within two hours, whereby the same conditions apply as in the case of the additional supply. See Figure 6 for an illustration.

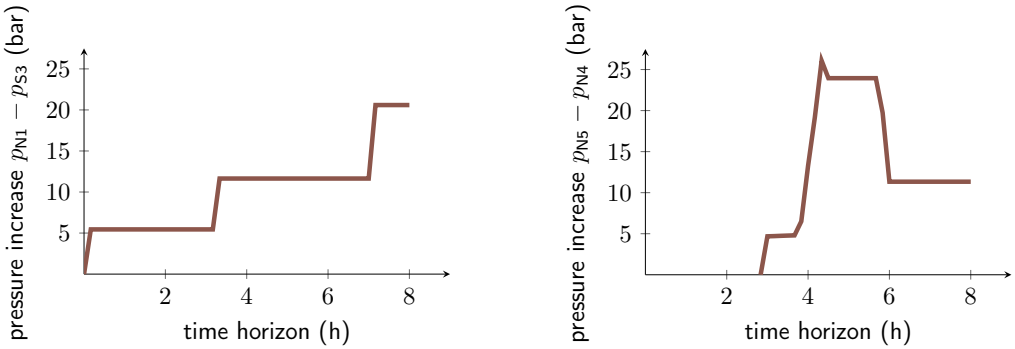

Figure 7. Profile for the pressure increase of compressor Cm1 (left) and compressor Cm2 (right) corresponding to the best solution for the storage capacity maximization problem (49) found after a total runtime of 4 h.

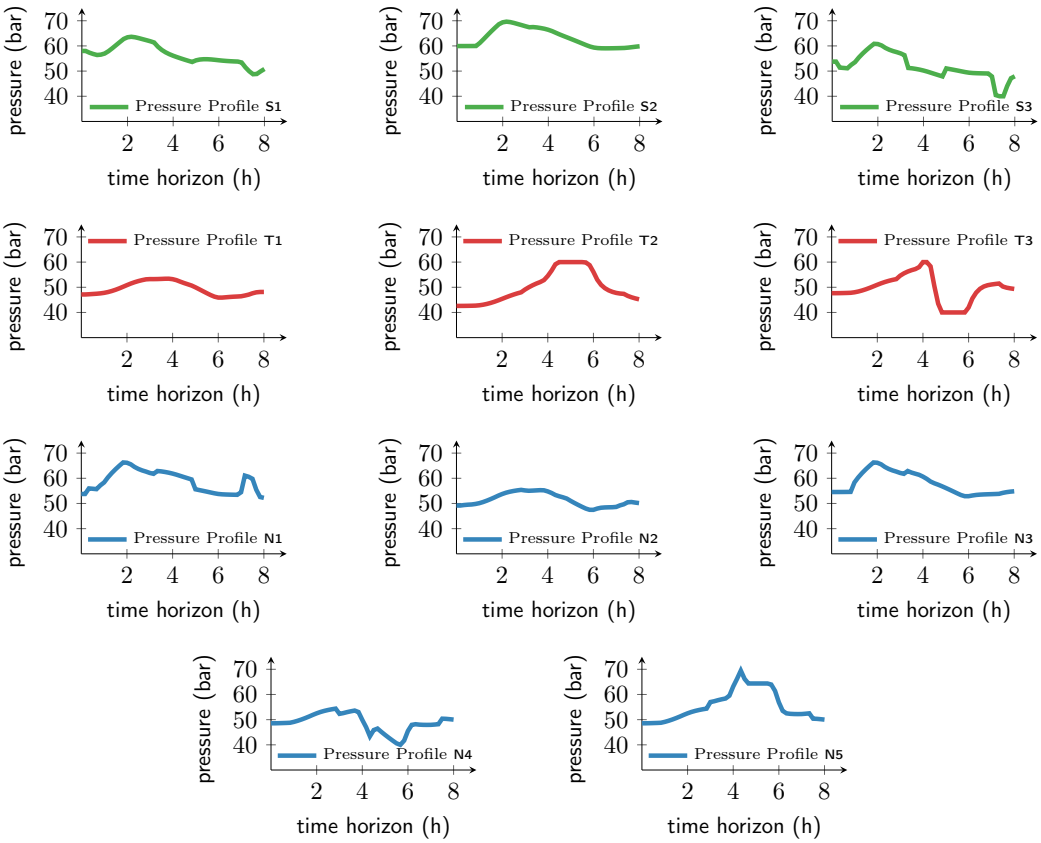

Figure 8. Profiles for the pressures of all eleven vertices of the GasLib-11 network in Figure 3. The values correspond to the best solution for the storage capacity maximization problem (49) found after a total runtime of 4 h.

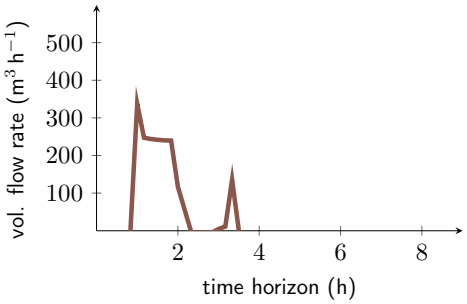

Figure 9. Volumetric flow rate profile for the valve Vl1 showing the amount of gas passing through the valve in case that it is open. The values correspond to the best solution for the storage capacity maximization problem (49) found after a total runtime of 4 h.

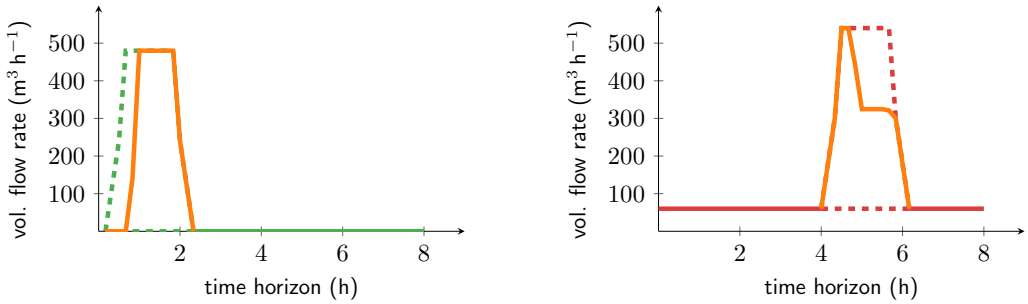

Figure 10. Volumetric flow rate profiles for the entry S1 (left) and the exit T2 (right) showing the additional amount of gas q^{extra} (orange) that is injected (S1) and discharged (T3). The values correspond to the best solution for the storage capacity maximization problem (49) found after a total runtime of 4 h.

After a total runtime limit of 4 h, the MIP-based approach delivers a feasible solution for the storage capacity maximization problem (49) that is globally optimal within a relative gap of almost 5 %. The corresponding profiles of the solution are shown in Figure 7 for the compressors Cm1 and Cm2, in Figure 8 for the pressures of all eleven vertices, in Figure 9 for the valve Vl1, and in Figure 10 for the additional amount of gas q^{extra}.

The compressor Cm1 is immediately switched on and operates throughout the whole time horizon. From minute 50 onwards, almost as much additional Gas q^{extra} is injected at S3 as possible. As a consequence, all pressure values rise with a higher amount of gas until no additional gas is injected in S3 anymore. Moreover, the valve Vl1 is opened, with approximately half of q^{extra} passing through it. About an hour before the additionally injected amount of gas is discharged at T3, the Compressor Cm2 is also switched on. At the same time, a small amount of gas passes through the valve again before it is closed. Due to the coincident compression of both compressors, the pressure at T3 remains within the pressure bounds while discharging the additional amount of gas.

Returning to the objective of maximizing the storage capacity, around 74.17 % of the possible additional amount of gas in q^{extra} is attainable according to our solution; see Figure 10. Due to the chosen parameters γ_1 and γ_2, the cost of compression is almost negligible in our MINLP problem. Furthermore, our solution is globally optimal within a

gap of less than 6 %. Hence, we conclude that taking into account the model from above, no more than approximately 78.62 % of the possible additional amount of gas in q^{extra} can be injected at S3.

Table 3. Iteration log of LaMaTTO++ for the storage capacity maximization problem (49) using the gas network in Figure 3 with a total runtime limit of 4 h.

iteration	dual	primal	gap	elapsed time
1	498.342	449.080	10.97 %	9.64
6	498.342	460.562	8.20 %	38.36
201	497.297	460.562	7.98 %	1726.50
218	494.919	460.562	7.46 %	1949.03
236	491.733	460.562	6.77 %	2216.00
237	490.160	460.562	6.43 %	5517.05
238	490.160	464.529	5.52 %	10 656.86
239	490.160	464.529	5.52 %	14 103.06

Finally, we show an iteration log of LaMaTTO++ for the storage capacity maximization problem (49) in Table 3. After a total runtime of less than 3 h, LaMaTTO++ is able to find a solution that is feasible for the storage capacity maximization problem (49) and globally optimal within a relative gap of almost 5 %.

As mentioned before, the MIP relaxation approach we utilize to solve our MINLP, adaptively refines MIP relaxations of the MINLP. The first column in Table 3 indicates the corresponding MIP relaxation. The best dual bound d of the MINLP and the objective value z of the incumbent (feasible) solution are given in column two and three, respectively. The next column contains the relative gap $|(z - d)/z|$, which is given in percent. The last column presents the runtime in seconds that LaMaTTO++ spent until the current iteration. We see that even with shorter runtime, LaMaTTO++ is able to find solutions with small relative gaps.

For the sake of comparison, the state-of-the-art MINLP solvers Baron and SCIP have the same MINLP solved on the same cluster using 12 cores and a runtime limit of 4 h. After the time limit has been reached, the best feasible solution Baron finds has an objective value of 332.991, while the best dual bound is 630.965. This translates into a relative gap of about 89 %. The best feasible solution SCIP finds has an objective value of 296.724, where the best dual bound is 622.838. This corresponds to a relative gap of about 109 %. The extended MIP-based approach of Burlacu et al., 2017; Geißler et al., 2012; Geißler, 2011 thus delivers significantly better results in this case.

In conclusion, we see that our time-expanded graph method can be successfully applied in the context of the storage capacity maximization of gas networks. In addition, the approach delivers solutions within reasonable runtime that are both physically plausible and near-global optimal.

6. Conclusion

In this paper, we presented a first-discretize-then-optimize approach for the maximization of the storage capacity of gas networks that are described by a coupled system of parabolic

PDEs and include active elements like valves and compressors. The main focus of our work is on global optimal solutions, including discrete decisions that result from switching active elements. To this end, we proposed a new discretization of the system of parabolic PDEs and proved well-posedness for the resulting nonlinear discretized system. Endowed with this discretization, we used a time-expanded graph method to model the problem of maximizing the storage capacity as a non-convex MINLP.

Moreover, we algorithmically extended the MINLP solver proposed by Burlacu et al., 2017; Geißler et al., 2012; Geißler, 2011, which has so far been used successfully for stationary gas transport optimization. We utilized this augmented MINLP solver to illustrate the applicability of our approach in a case study yielding both physically plausible and near-global optimal solutions. In addition, our method was able to find high-quality solutions even at short runtime. We therefore believe that our time-expanded graph approach is also suitable for the global optimization of other difficult problems in the field of transient gas transport optimization, which involve discrete decisions. Examples include problems with more realistic compressor models or large-scale time horizons of several days, which is part of our future work.

Acknowledgements

The authors thank the Deutsche Forschungsgemeinschaft for their support within Projects A05, A07, B07, B08, and C04 of the Sonderforschungsbereich/Transregio 154 "Mathematical Modelling, Simulation and Optimization using the Example of Gas Networks". Part of the research was performed at the Energie Campus Nürnberg and supported by funding through the "Aufbruch Bayern (Bavaria on the move)" initiative of the state of Bavaria. The authors gratefully acknowledge the compute resources and support provided by the Erlangen Regional Computing Center (RRZE). We are very grateful for the thorough reading of the paper by Martin Schmidt. We would also like to show our gratitude to Fabian Rüffler for fruitful discussions on the topic of discretization of PDEs. Finally, we thank Falk Hante for his helpful comments on the literature review of the general approaches for optimal control with discrete decisions.

References

A. J. Osiadacz (1996). *Different transient models – limitations, advantages and disadvantages*. Tech. rep. PSIG report 9606, Pipeline Simulation Interest Group.

Allgor, R. and P. Barton (1999). "Mixed-integer dynamic optimization I: problem formulation". In: *Computers & Chemical Engineering* 23.4, pp. 567–584. DOI: 10.1016/S0098-1354(98)00294-4.

Baumrucker, B. and L. Biegler (2009). "MPEC strategies for optimization of a class of hybrid dynamic systems". In: *Journal of Process Control* 19.8. Special Section on Hybrid Systems: Modeling, Simulation and Optimization, pp. 1248–1256. DOI: 10.1016/j.jprocont.2009.02.006.

Belotti, P., C. Kirches, S. Leyffer, J. Linderoth, J. Luedtke, and A. Mahajan (2013). "Mixed-integer nonlinear optimization". In: *Acta Numerica* 22, pp. 1–131. DOI: 10.1017/S0962492913000032.

Bock, H. G., C. Kirches, A. Meyer, and A. Potschka (2018). "Numerical solution of optimal control problems with explicit and implicit switches". In: *Optimization Methods and Software* 33.3, pp. 450–474. DOI: 10.1080/10556788.2018.1449843.

Buchheim, C., R. Kuhlmann, and C. Meyer (2015). *Combinatorial Optimal Control of Semilinear Elliptic PDEs*. Tech. rep. Optimization Online. URL: http://www.optimization-online.org/DB_HTML/2015/10/5161.html.

Burlacu, R., B. Geißler, and L. Schewe (2017). *Solving Mixed-Integer Nonlinear Programs using Adaptively Refined Mixed-Integer Linear Programs*. Preprint. URL: http://www.optimization-online.org/DB_HTML/2017/05/6029.html.

Domschke, P., B. Geißler, O. Kolb, J. Lang, A. Martin, and A. Morsi (2011). "Combination of Nonlinear and Linear Optimization of Transient Gas Networks". In: *INFORMS Journal on Computing* 23.4, pp. 605–617. DOI: 10.1287/ijoc.1100.0429.

Domschke, P., B. Hiller, J. Lang, and C. Tischendorf (2017). *Modellierung von Gasnetzwerken: Eine Übersicht*. Techreport. URL: https://opus4.kobv.de/opus4-trr154/frontdoor/index/index/docId/191 (visited on 06/25/2018).

Fügenschuh, A., B. Geißler, R. Gollmer, A. Morsi, M. E. Pfetsch, J. Rövekamp, M. Schmidt, K. Spreckelsen, and M. C. Steinbach (2015). "Physical and technical fundamentals of gas networks". In: *Evaluating Gas Network Capacities*. Ed. by T. Koch, B. Hiller, M. E. Pfetsch, and L. Schewe. SIAM-MOS series on Optimization. SIAM. Chap. 2, pp. 17–43. DOI: 10.1137/1.9781611973693.ch2.

Gamrath, G., T. Fischer, T. Gally, A. M. Gleixner, G. Hendel, T. Koch, S. J. Maher, M. Miltenberger, B. Müller, M. E. Pfetsch, C. Puchert, D. Rehfeldt, S. Schenker, R. Schwarz, F. Serrano, Y. Shinano, S. Vigerske, D. Weninger, M. Winkler, J. T. Witt, and J. Witzig (2016). *The SCIP Optimization Suite 3.2*. eng. Tech. rep. 15-60. Takustr.7, 14195 Berlin: ZIB.

GAMS (2017). *General Algebraic Modeling System (GAMS) Release 24.8.3*. Washington, DC, USA. URL: http://www.gams.com/.

Geißler, B. (2011). "Towards Globally Optimal Solutions of MINLPs by Discretization Techniques with Applications in Gas Network Optimization". PhD thesis. FAU Erlangen-Nürnberg.

Geißler, B., A. Martin, A. Morsi, and L. Schewe (2012). "Using Piecewise Linear Functions for Solving MINLPs". In: *Mixed Integer Nonlinear Programming*. Ed. by J. Lee and S. Leyffer. Springer New York, pp. 287–314.

– (2015a). "The MILP-relaxation approach". In: *Evaluating Gas Network Capacities*. Ed. by T. Koch, B. Hiller, M. E. Pfetsch, and L. Schewe. SIAM-MOS series on Optimization. SIAM. Chap. 6, pp. 103–122. DOI: 10.1137/1.9781611973693.ch6.

Geißler, B., A. Morsi, L. Schewe, and M. Schmidt (2015b). "Solving power-constrained gas transportation problems using an MIP-based alternating direction method". In: *Computers & Chemical Engineering* 82, pp. 303–317. DOI: 10.1016/j.compchemeng.2015.07.005.

– (2018). "Solving Highly Detailed Gas Transport MINLPs: Block Separability and Penalty Alternating Direction Methods". In: *INFORMS Journal on Computing* 30.2, pp. 309–323. DOI: 10.1287/ijoc.2017.0780.

Gerdts, M. (2006). "A variable time transformation method for mixed-integer optimal control problems". In: *Optimal Control Applications and Methods* 27.3, pp. 169–182. DOI: 10.1002/oca.778.

Gu, Z., E. Rothberg, and R. Bixby (2015). *Gurobi Optimizer Reference Manual, Version 6.0.4*. Houston, Texas, USA: Gurobi Optimization Inc.

Gugat, M., G. Leugering, A. Martin, M. Schmidt, M. Sirvent, and D. Wintergerst (2017). "MIP-Based Instantaneous Control of Mixed-Integer PDE-Constrained Gas Transport Problems". In: *Computational Optimization and Applications*. DOI: 10.1007/s10589-017-9970-1.

Hahn, M., S. Leyffer, and V. M. Zavala (2017). *Mixed-Integer PDE-Constrained Optimal Control of Gas Networks*. Techreport. URL: https://wiki.mcs.anl.gov/leyffer/images/2/27/GasNetMIP.pdf (visited on 06/25/2018).

Hante, F. M. and S. Sager (2013). "Relaxation methods for mixed-integer optimal control of partial differential equations". In: *Computational Optimization and Applications* 55.1, pp. 197–225. DOI: 10.1007/s10589-012-9518-3.

Hante, F., G. Leugering, A. Martin, L. Schewe, and M. Schmidt (2017). "Challenges in optimal control problems for gas and fluid flow in networks of pipes and canals: From modeling to industrial applications". In: *Industrial Mathematics and Complex Systems*. Ed. by P. Manchanda, R. Lozi, and A. H. Siddiqi. Industrial and Applied Mathematics. Springer, pp. 77–122. DOI: 10.1007/978-981-10-3758-0_5.

J. Brouwer, I. Gasser, and M. Herty (2011). "Gas pipeline models revisited: Model hierarchies, nonisothermal models, and simulations of networks". In: *Multiscale Modeling and Simulation* 9, pp. 601–623. DOI: 10.1137/100813580.

Jung, M. N., G. Reinelt, and S. Sager (2015). "The Lagrangian relaxation for the combinatorial integral approximation problem". In: *Optimization Methods and Software* 30.1, pp. 54–80. DOI: 10.1080/10556788.2014.890196.

Koch, T., B. Hiller, M. E. Pfetsch, and L. Schewe, eds. (2015). *Evaluating Gas Network Capacities*. SIAM-MOS series on Optimization. SIAM. xvii + 364. DOI: 10.1137/1.9781611973693.

LaMaTTO++ (2015). *A Framework for Modeling and Solving Mixed-Integer Nonlinear Programming Problems on Networks*. URL: www.mso.math.fau.de/edom/projects/lamatto.html.

Lee, H., K. Teo, V. Rehbock, and L. Jennings (1999). "Control parametrization enhancing technique for optimal discrete-valued control problems". In: *Automatica* 35.8, pp. 1401–1407. DOI: 10.1016/S0005-1098(99)00050-3.

Lee, J. and S. Leyffer, eds. (2012). *Mixed integer nonlinear programming*. Vol. 154. The IMA Volumes in Mathematics and its Applications. Selected papers based on the IMA Hot Topics Workshop "Mixed-Integer Nonlinear Optimization: Algorithmic Advances and Applications" held in Minneapolis, MN, November 17–21, 2008. Springer, New York, pp. xvii+690.

Mahlke, D., A. Martin, and S. Moritz (2010). "A mixed integer approach for time-dependent gas network optimization". In: *Optimization Methods and Software* 25.4, pp. 625–644. DOI: 10.1080/10556780903270886.

Ríos-Mercado, R. Z. and C. Borraz-Sánchez (2015). "Optimization problems in natural gas transportation systems: A state-of-the-art review". In: *Applied Energy* 147, pp. 536–555. DOI: 10.1016/j.apenergy.2015.03.017.

Rüffler, F. and F. M. Hante (2016). "Optimal switching for hybrid semilinear evolutions". In: *Nonlinear Analysis: Hybrid Systems* 22, pp. 215–227. DOI: 10.1016/j.nahs.2016.05.001.

Sager, S., H. G. Bock, and G. Reinelt (2009). "Direct methods with maximal lower bound for mixed-integer optimal control problems". In: *Mathematical Programming* 118.1, pp. 109–149. DOI: 10.1007/s10107-007-0185-6.

Sager, S., M. Jung, and C. Kirches (2011). "Combinatorial integral approximation". In: *Mathematical Methods of Operations Research* 73.3, pp. 363–380. DOI: 10.1007/s00186-011-0355-4.

Schmidt, M., D. Aßmann, R. Burlacu, J. Humpola, I. Joormann, N. Kanelakis, T. Koch, D. Oucherif, M. E. Pfetsch, L. Schewe, R. Schwarz, and M. Sirvent (2017). "GasLib—A Library of Gas Network Instances". In: *Data* 2.4. DOI: 10.3390/data2040040.

Tawarmalani, M. and N. V. Sahinidis (2005). "A polyhedral branch-and-cut approach to global optimization". In: *Mathematical Programming* 103 (2), pp. 225–249. DOI: 10.1007/s10107-005-0581-8.